The impact of El Niño Southern Oscillation on cropping season rainfall variability across Central Brazil

Citation:

Heinemann, A.B.; Ramirez-Villegas, J.; Stone, L.F.; Garcia Abreu Silva, A.P.; Henriques da Matta, D.; Piscoya Diaz, M.E. (2020) The impact of El Niño Southern Oscillation on cropping season rainfall variability across Central Brazil, Online first paper (29 May 2020) ISSN: 0899-8418

Publisher's DOI:
https://doi.org/10.1002/joc.6684

Access through CIAT Research Online:
https://hdl.handle.net/10568/108999

The impact of El Niño Southern Oscillation on cropping season rainfall variability across Central Brazil

Alexandre Bryan Heinemann[1]*, Julian Ramirez-Villegas[2,3], Luís Fernando Stone[1], Ana Paula Garcia Abreu Silva[4], David Henriques da Matta[4] and Mario Ernesto Piscoya Diaz[4]

[1]Embrapa Arroz e Feijão Rodovia GO-462 km 12 Zona Rural, 75375-000 Santo Antônio de Goiás, GO, Brazil, e-mail: alexandre.heinemann@embrapa.br; luis.stone@embrapa.br

[2] International Center for Tropical Agriculture (CIAT), Km. 17 Recta Cali-Palmira A.A. 6713, Cali, Colombia, e-mail: j.r.villegas@cgiar.org

[3] CGIAR Research Program on Climate Change, Agriculture and Food Security (CCAFS), c/o CIAT, Cali, Colombia

[4] Federal University of Goiás (UFG), Institute of Mathematics and Statistics (IME), Campus II - Av. Esperança, s/n Instituto de Matemática e Estatística, Samambaia, Goiânia GO, 74001-970, e-mail: apestatistica@outlook.com; davidhmatta@gmail.com; mario.piscoya@gmail.com

[*]Correspondence: alexandre.heinemann@embrapa.br; Tel: +55 62 35332153

Highlights

- We analyzed the impact of ENSO (El Niño Southern Oscillation) on the growing season characteristics of Central Brazil.
- The length of the sowing period is markedly reduced during La Niña years across the region.
- We propose a mean optimal crop sowing calendar for Central Brazil based on crop modeling results of ENSO effects.

Keywords

Rainfall; Growing season; Rice; Brazil; Crop modeling.

Abstract

Local-level understanding of within-season rainfall variability and its relationship with the El Niño Southern Oscillation (ENSO) can shed light on crop yield variations and establish appropriate cropping calendars in rainfed systems. This requires information on the growing season, including its length, the total rainfall, the onset and cessation of rainfall, the number of wet and dry days, and the optimal sowing window. The objective of this study was to examine the onset and cessation of both the rainy and growing seasons using historical daily rainfall datasets (1980–2013) from 50 weather stations distributed across the main grain production region of Brazil. We then correlated the interannual variability of the climate variables and crop water availability with ENSO (using the Oceanic Niño Index, ONI). Across the study region, the onset of the rainy period ranged from late September to early November, and the cessation period ranged from late March to mid-April. The onset of the growing season followed that of the rainy season, beginning across central and northern Mato Grosso in mid-October, followed by Goiás and Tocantins, and finally Rondônia by the end of October. The length of the sowing window was reduced, and the mean optimal sowing date was delayed during La Niña years for most weather stations in the study region. Our results infer the need to adjust the cropping calendars for specific ENSO phases only in regions that conduct crop rotations. Based on rice crop model simulations of water availability, we propose a mean optimal crop sowing calendar for annual crops in Central Brazil.

1. Introduction

In the 2017/2018 production season, Brazil produced an estimated 229.7 million tons (8.64% of the world's production) of grains across a total area of 61.6 million hectares (CONAB, 2018). The primary region of grain (mainly soybean and maize) production in the country is Central Brazil, and agricultural expansion in this region over the last three decades was driven largely by the international commodity market (Verburg *et al.*, 2014a, b). The states of Mato Grosso, Goiás, Rondônia, and Tocantins, located in this region, harbor 37 % of the country's total grain cropped area (39% of the grain production) (CONAB, 2018). Mato Grosso has the largest cropped area and grain production, followed by Goiás, Tocantins, and Rondônia. Regional farming and production is highly dependent on the rainy season. Therefore, precipitation variability significantly affects the socio-economic well-being of the region's population, as their livelihoods and food security are dependent on these rainfed crop systems (PBMC, 2014; Abrahão and Costa, 2018).

The relationships between tropical Pacific sea surface temperatures (SSTs), the El Niño Southern Oscillation (ENSO), and regional climate variability across the world are well established (Coelho *et al.*, 2002; Grimm and Tedeschi, 2009; Carvalho *et al.*, 2011). In particular, a number of studies have demonstrated a link between ENSO and regional climate variability of northeastern (Liu and Juárez, 2001; Rodrigues *et al.*, 2011; Moura *et al.*, 2019), southeastern (Carvalho *et al.*, 2004), and southern (Grimm and Pscheidt, 2001; Gelcer *et al.*, 2013) regions of Brazil, in which the likelihood of abnormal flooding in the south and intense droughts in the north/northeast were found to be significantly higher during El Niño (warm ENSO phase) events. The opposite was observed during La Niña (cold ENSO phase) events, while Central Brazil was classified as a transitional region (Grimm, 2003; Penalba and Rivera, 2016; Moura *et al.*, 2019; Nóia Júnior and Sentelhas, 2019a). Many studies have also assessed the impacts of ENSO on climate and crop productivity during the growing season on global and regional scales (Fraisse *et al.*, 2008; Iizumi *et al.*, 2014; Liu *et al.*, 2014; Battisti *et al.*, 2018a, b; Nóia Júnior and Sentelhas, 2019a).

However, there is a lack of studies on the impacts of ENSO on precipitation during the crop-growing season in Central Brazil, despite the region's high crop production. Moreover, the links between within-season precipitation variability and agricultural activities have not been considered in previous investigations (e.g., Marengo *et al.*, 2001; Liebmann *et al.*, 2007; Debortoli *et al.*, 2015). Local characteristics of within-season rainfall variability (e.g., amount of rainfall, onset and cessation of rainfall, number of rainy days, the length of the growing season, and optimal sowing windows), their relationship with ENSO, and its effects on the seasonal distribution of water are crucial toward understanding crop yield variations in rainfed systems (e.g., Delerce *et al.*, 2016; Iizumi *et al.*, 2014). Information on these variables helps to improve upon existing cropping calendars and develop new cropping systems and strategic sowing management options (Nóia Júnior and Sentelhas, 2019b). Understanding within-season precipitation variability can also indicate the climatic suitability for a given crop (Araya *et al.*, 2010; Zabel *et al.*, 2014; Rippke *et al.*, 2016), or help to determine geographic domains for yield gap assessments and agronomic management (van Wart *et al.*, 2015). This can also further address the issue of food security by more adequately assessing seasonal and geographic variations in grain supply to mitigate shortages at certain times of the year (Mishra *et al.*, 2008; Paeth *et al.*, 2008; Simelton, 2011). Moreover, determining the onset, cessation, and length of the growing season and their links to ENSO are useful for quantifying the potential risks of abiotic and biotic stresses during the cropping season. This information can be applied in breeding programs to develop new varieties for a specified target environment.

The main objective of this study was to examine the interannual variability in the onset and cessation of the rainy and growing seasons in response to ENSO across Brazil's primary grain production region. We proposed a mean optimal crop sowing calendar based on an assessment of water availability across the region. The specific objectives are as follows:

(i) to determine the mean onset, cessation, length, number of dry and wet days, and amount of precipitation during the rainfall and growing seasons,

(ii) to assess the effect of ENSO on the abovementioned rainy and growing season variables,

(iii) to analyze the dynamics of crop water utilization during the growing season. We propose a mean optimal sowing windows based on the ratios of actual to potential transpiration using a crop model simulation.

Finally, we discuss our findings in the context of taking pre-emptive measures to reduce climate risks on crop production in Brazil's highest grain production region.

2. Materials and Methods

2.1. Regional setting

The study area covers part of the Cerrado biome (the states of Goiás, south of Mato Grosso, and Tocantins) and the transition zone between the Amazon and the Cerrado biomes (states of Rondônia, north of Mato Grosso, and Tocantins). The region has a surface area of ca. 1.76 million km^2, with an altitude, latitude, and longitude range of 300–900 m above mean sea level, 20º (S) to 5º (S), and 61º (W) to 46º (W) (Figure 1), respectively. The predominant climate in the region is tropical savanna (Aw), which represents 100%, 94%, and 52.8% of the total area of Tocantins, Goiás, and Mato Grosso, respectively (Alvares *et al*., 2013). Rondônia (100%) and the north of Mato Grosso (47.2%) have tropical monsoon (Am) climates. The region's rainfall regime shows strong seasonality (monomodal pattern) with only two seasons (wet and dry). More than 80 % of the total annual rainfall occurs in the wet season, between October and March, with highest rainfall from January to March. In contrast to the equatorial northern part of the Amazon basin, which has a relatively short dry season (Marengo, 2006), the dry period in the study region typically lasts from April to September (e.g., Funatsu *et al.*, 2012). The annual rainfall in the study region ranges from 1,300 (Aw) to 2,300 mm (Am climate, Rondônia and north of Mato Grosso).

2.2. Meteorological data

We used time series datasets of daily rainfall obtained from the Brazilian Institute of Meteorology (INMET). Fifty meteorological stations were selected to represent the entire study region (Figure 1). We obtained continuous meteorological records spanning 1980–2013 (33 years) from each station. These datasets were quality controlled, checked for homogeneity, and gap-filled to address missing data and possible outliers due to human-induced error or faulty measuring equipment (Ramirez-Villegas and Challinor, 2012; Van Wart *et al*., 2015). To fill the gaps in the dataset, we gathered data from two databases: the Agência Nacional de Águas, Brazil (ANA, https://www.ana.gov.br/gestao-da-agua/sistema-de-gerenciamento-de-recursos-hidricos/agencias-de-agua) and the Climate Prediction Center (CPC, https://www.cpc.ncep.noaa.gov/). ANA is a database of weather station data, whereas CPC provides gridded data. We used the ANA data to the maximum extent and only used the CPC data to fill in missing ANA entries. We ran visual checks of the final time series dataset (1980–2013) to ensure the data was free of implausible characteristics. The "gap-filling" method is described in detail in Ramirez-Villegas *et al.* (2018) and Heinemann *et al.* (2019). Missing rainfall data at most stations occurred in approximately 20% of the total number of days.

2.3. ENSO data

ENSO conditions are typically defined by sea surface temperature (SST) variations and their persistence along the equatorial Pacific Ocean (NOAA, 2019). The National Oceanic and Atmospheric Administration (NOAA) defines El Niño and La Niña events based on a threshold temperature anomaly of ± 0.5 ºC on the Oceanic Niño Index (ONI), which in turn is computed as the 3-month running mean of SST anomalies across the Eastern Equatorial Pacific (Bhuvaneswari *et al*., 2013). As the rainfall season occurs between September and March in the study region, we averaged the ONI values from September, October, and November (SON) to February, March, and April (FMA). For the purpose of our analysis, values lower than -0.5 ºC are considered La Niña years, values higher than 0.5 ºC are considered El Niño years, and -0.5–0.5 ºC are considered Neutral (NOAA, 2019).

2.4. Rainy season onset and cessation criteria

To assess within-season precipitation variations for the study region, we first determined the onset and cessation of the rainy season. We employed the method described by Liebmann *et al.* (2007, 2012) to produce a precipitation climatology for the entire study region. This method has been previously used on observational datasets over northern Brazil (Liebmann *et al.*, 2007), Mato Grosso (Arvor *et al.*, 2014), the southern Amazon (Debortoli *et al.*, 2015), and Africa (Dunning *et al.*, 2016). A cumulative daily precipitation anomaly (*AA*, mm) over time was defined for each weather station (Table 1) following Equation 1:

$$AA = \sum_{n=1}^{day}[R(n) - \bar{R}], \qquad \text{eq. 1}$$

where *R(n)* is the daily precipitation (mm day^{-1}) on day *n* from 1980 to 2013, $\bar{R}$ is the climatological mean daily rainfall (mm) for the year as a whole. In the entire study region, the 1st of July is always within the first half of the dry period, so we started the calculation on this date (Funatsu *et al.*, 2012), as there are no ENSO influences on the rainy period during this time. Large-scale precipitation in the region occurs exclusively with the passage of cold fronts (Li and Fu, 2006).

The onset (RS_{START}) and cessation (RS_{END}) dates are determined by identifying the minima and maxima in the cumulative daily precipitation anomaly, respectively, which increases when the daily precipitation is above the climatological mean daily rainfall and decreases when it is below the climatological mean daily rainfall (Supplementary Figure S1). An advantage of this method is that it does not incorporate external parameters, such as the pentads method, which can be highly sensitive to the chosen threshold (see Liebmann and Marengo, 2001; Marengo *et al.*, 2001). The total precipitation amount (RS_{TPA}) during the rainy season was calculated by the precipitation sum between RS_{START} and RS_{END}. The length of the rainy season (RS_L) was calculated by the difference (in days) between the cessation (RS_{END}) and onset (RS_{START}) dates of the rainfall season. Finally, the number of dry (RS_{NDD}) and wet days (RS_{NWD}) were calculated based on the number of days above (wet) or below (dry) 0.1 mm day^{-1} of rainfall between RS_{START} and RS_{END}. Days with exactly 0.1 mm day^{-1} were considered dry. We selected a threshold of 0.1 mm day^{-1}, as it is the typical precision of rain gauge measurements (Mathugama and Peiris, 2011). Algorithms were written for automatically determining the RS_{START}, RS_{END}, RS_{TPA}, RS_L, RS_{NDD}, and RS_{NWD} for each year and for each weather station.

For a descriptive analysis, the RS_{START}, RS_{END}, RS_{TPA}, RS_{L}, RS_{NDD}, and RS_{NWD} values were averaged for each weather station. Before averaging, we eliminated all potential outliers, which were defined as values >1.5 times the interquartile range. The mean values of the variables were interpolated and rasterized in the study region to show the geographic variation of each variable. For interpolation, we applied the Inverse Distance Weighting (IDW) method with the "Shepherd" algorithm and a power parameter setting of two. The IDW was selected because it is a deterministic method for multivariate interpolation with a known scattered set of points. The IDW spatial interannual variability (expressed as the standard deviation) and accuracy (expressed as the root mean square error, RMSE) are shown in the Supplementary Information (Figures S2, S3 and Table S2). We rasterized the IDW output following interpolation, assuming that x, y are the centers of the cells with a spatial resolution equal to the minimum distance between any pair of weather stations. For rasterization, we used the "idw" and "rasterFromXYZ" functions from the gstat (Gräler *et al.*, 2016) and raster (Hijmans and van Etten, 2012) R packages.

2.5. Growing season onset criteria

We determined the crop-growing season following the establishment of RS_{START} and RS_{END}. The growing season onset (GS_{START}) is defined as the period during the rainy season when rainfall is sufficient for crop sowing, germination, establishment, and full development (Odekunle, 2004). There are several methods for determining GS_{START} (Marteau *et al.*, 2011; Ngetich *et al.*, 2014; Oguntunde *et al.*, 2014), the criteria of which depend on subjective thresholds, such as the amount of accumulated rainfall. According to the American soil classification (texture), the most relevant soil types in our study region are Oxisols with sandy loam texture, followed by sandy clay loam and clay textured Oxisols (Heinemann *et al.*, 2015). For these soil types, a total rainfall amount of 33 mm in four consecutive days is sufficient to bring the first layer (~17 cm) of soil to field capacity for sowing. These parameters may vary with factors such as management practices and plant drought tolerance. However, the values used in this study are considered conservative for common soils, and management practices in Brazil. To avoid determining false growing season onsets due to drought spells at the beginning of the rainy season, GS_{START} is only defined when a total rainfall amount of 33 mm occur in four consecutive days and when at least 10 mm of rainfall occur in the first 10 days after this period, with 5 mm distributed in the first 5 days and the other 5 mm distributed in the following 5 days. The criteria for defining GS_{START} are summarized below:

a) occurring within the rainfall season;
b) a total rainfall of 33 mm between the first and fourth day;
c) 5 mm of rainfall from the fifth to the ninth day; and,
d) 5 mm of rainfall from the tenth to the fourteenth day.

Thus, a growing season is defined if a total of 43 mm of accumulated rainfall has occurred over 14 consecutive days. In this study, we considered the cessation of the growing season (GS_{END}) to be the same as the cessation of the rainfall season (GS_{END} = RS_{END}). The number of dry (GS_{NDD}) and wet days (GS_{NWD}) in the growing season were computed as the number of days above (wet) or below (dry) a rainfall amount of 0.1 mm between GS_{START} and GS_{END} (also see Sect. 2.3). The values of GS_{START}, GS_{NDD}, and GS_{NWD} were then averaged per station and subsequently interpolated to produce geographic maps following the method described in Sect. 2.4.

2.6. Determining ENSO influences on the characteristics of the rainy and growing seasons

In this study, we assessed the relationship between ENSO (La Niña/El Niño years) and the characteristics of the rainy and growing seasons. For discrete variables (RS_{START}; RS_{END}; RS_{L}; RS_{NDD}; RS_{NWD}; GS_{START}; GS_{NWD}; and GS_{NDD}), we applied generalized linear models (GLM) with four discrete family distributions: 1) Poisson regression, 2) negative binomial regression, 3) Poisson regression (longitudinal dataset), and 4) negative binomial regression (longitudinal dataset). For the continuous variable RS_{TPA}, we applied three statistical models: 1) multiple linear regression, 2) a mixed linear model, and 3) a longitudinal random effects model (intercept model). For all models, ENSO (anomalies El Niño/La Niña/Neutral; Sect. 2.3), the state, and their interaction (ENSO*state) were considered as a qualitative fixed effect. When the respective model framework allowed it, weather station identification (Figure 1 and Table 1) were tested as random effects (with random intercepts and fixed predictors at the individual level). We considered the Bayesian information criterion (BIC) as the criterion for best fit. All statistical analyses were conducted using STATA v.13 software.

2.7. Sowing window calendar in the growing season and its viability

We produced a sowing window calendar for each state and weather station based on the ENSO influence on GS_{START} (Sect. 2.5). The multi-year (1980–2013) mean GS_{START} was defined as the mean optimal sowing date, and the starting (end) of the sowing window was defined as the mean GS_{START} minus (plus) the standard deviation. To verify the viability of the sowing window calendar (starting, optimal, and end), we applied the ORYZA v3 (Li *et al.*, 2017) crop model to assess the crop water use dynamics of upland rice. Upland rice cultivar BRS Primavera was specifically chosen, as the crop is drought sensitive and cultivated in the study region (Heinemann *et al.*, 2019). Water use dynamics were assessed using the temporal variability of the ratios of the five-day moving averages of actual to potential transpiration (PCEW, daily crop model output). In the model, this acts as a daily photosynthesis reduction factor—from crop emergence to 30 days after emergence (DAE)—for each weather station and year in the period 1980–2013. We also determined the accumulated rainfall at 15 and 30 days after sowing for starting, optimal, and end dates for each weather station and each year.

For each weather station and year (1980–2013), the ORYZA v3 model was used to simulate the starting, mean optimal, and end sowing dates throughout the first 30 days of upland rice development and growth. We used historical daily weather data from 1980–2013 (precipitation, maximum and minimum temperature, and downward shortwave solar radiation) as the input to the crop model. The gap-filling procedure for precipitation is described in Sect. 2.2. The daily solar radiation for all weather stations, except for the station in Santo Antônio de Goiás (Lat: -16.47; Long: -49.28, ID 2, Table 1), was estimated according to the method by Richardson and Wright (1984). The maximum and minimum temperatures were averaged when the data gap was less than or equal to 2 days. The CPC dataset was used for data gaps of >2 days. We conducted visual checks of the finalized time series (1980–2013) to ensure that the data was free of errors or implausible characteristics.

The ORYZA v3 model parametrization (see Supplementary Figure S4) and evaluation of BRS Primavera upland rice cultivar are described in Heinemann *et al.* (2015) (also see Ramirez-Villegas *et al.*, 2018; Heinemann *et al.*, 2019). The ORYZA v3 crop model performance (simulated vs. measured for flowering; physiological maturation and yield for parameterization processes and panicle initiation; flowering and physiological maturation for evaluation processes of the BRS Primavera upland rice cultivar) is shown in the Supplementary Information (Figure S4). We used sandy loam for all simulations, as it is the most representative (Heinemann *et al.*, 2015) soil texture in the region (see Supplementary Table 1 for soil profile properties). We simulated water dynamics using the 'PADDY' soil water balance module. This is a one-dimensional multi-layer (up to 10) model that simulates the soil water balance for a variety of growing conditions (e.g., puddled or non-puddled), incorporating free or impeded drainage at particular depths in the soil profile. All simulations were rainfed, without biotic constraints and nitrogen limitations. All model runs were initiated in February, regardless of the sowing date, in order to establish realistic soil water profiles based on the rainfall patterns prior to the actual sowing date. Potential transpiration and evaporation rates were calculated based on the Priestley–Taylor method. The analysis of PCEW across the sowing dates and weather stations allowed us to verify the viability of the crop sowing calendar of the study region in response to ENSO.

3. Results

3.1 The spatial and seasonal variability of mean rainfall

The climatological mean daily rainfall ($\bar{R}$; Eq. 1) ranged from 3.45 to 5.59 mm, with an average value of 4.21 mm across all weather stations. $\bar{R}$ showed an increasing trend toward the equator (Figure 2) and was weakly positively correlated with latitude (Spearman's rho of 0.37) and weakly negatively correlated with longitude (Spearman's rho of -0.28) (also see Sect. 3.2).

For the descriptive analysis, only RS_{START}, RS_{L}, RS_{NDD} and RS_{NWD} variables presented outliers. The outliers represent only 5% for each variable.

3.1.1. Onset and cessation of the rainfall season

In the study region, RS_{START} ranged from late September (272 day of the year (DOY)) to early November (310 DOY), with an average onset date of October 25 (298 DOY, standard deviation (sd) = 7.4 DOY). We observed early onset dates (<280 DOY) in Mato Grosso, except in the south, and later onset dates (~300 DOY and later) in Rondônia, Tocantins, and Goiás (Figure 3A). Earlier onsets and late cessations were predominantly observed in forested regions, which is expected in Mato Grosso, despite continuous deforestation (Debortoli *et al.*, 2015). The onset orientation is related to the presence of the South Atlantic Convergence Zone (SACZ) in spring, which is influenced by the interactions between tropical convection systems and mid-latitude frontal systems (Gan *et al.*, 2004). The mean onset in Mato Grosso occurred around mid-October (18/10, 291 DOY, sd = 10.6 DOY). In agreement, satellite (Arvor *et al.*, 2014) and weather station data (Debortoli *et al.*, 2015) in Mato Grosso inferred a mean onset date of 18/10 (291 DOY) and 14/10 (288 DOY), respectively. The onset of the rainy season occurred at the end of October for Goiás, Rondônia, and Tocantins (298, 300, and 301 DOY, respectively).

In contrast to the 6-week duration of the onset period, RS_{END} only lasted 3 weeks across the entire region from late March (85 DOY) to mid-April (109 DOY), with an average end date at the beginning of April (96 DOY, sd = 5.9 DOY) (Figure 3B). In agreement, the standard deviation of the onset was greater than that of the cessation (Supplementary Figure S2A, B). The cessation starts in the southeast region (Goiás State) and gradually advances to the northwest, with the exception of north-west Mato Grosso, which experiences the earliest cessation (~85 DOY). State-wide averages infer earliest rainy season cessation in Goiás (beginning of April, 92 DOY, sd = 2.5 DOY), which extends to mid-April in Rondônia (99 DOY, sd = 2.3 DOY), Mato Grosso (101 DOY, sd = 6.4 DOY), and Tocantins (103 DOY, sd = 5.0). Overall, the spatial variability of RS_{END} can be explained by the northward shift of convection systems in connection with the Intertropical Convergence Zone (ITCZ) (Gan *et al.*, 2004). In agreement, Debortoli *et al.* (2015) and Arvor *et al.* (2014) determined a mean value of 95 DOY in the Cerrado of Mato Grosso and 90 DOY for the entire state of Mato Grosso, respectively.

3.1.2. Rainy season length and total rainfall

The RS_L ranged from 149 to 196 days across the study region, with an average of 164 days (sd = 10.8 days). The spatial variability of RS_L showed a northwest to southeast orientation (Figure 3C). The longest seasonal durations were observed within the central northern region to the south (within Mato Grosso), and decreased toward the southeast (Goiás). The highest average seasonal length was observed in Mato Grosso at 175 days (sd = 13.7 days), followed by Tocantins (168, sd = 8.2 days), Rondônia (164, sd = 11.1 days), and Goiás (159, sd = 6.7 days). In comparison, Arvor *et al.* (2014) inferred a mean value of 162 days for Mato Grosso. We observed lowest RS_L durations in Goiás. RS_L was found to strongly correlate with the onset (negatively) and cessation (positively) of the rainy season due to its northwest to southeast orientation (Figure 3C; see Sect. 3.2).

RS_{TPA} ranged from 1,038 to 1,723 mm across the study region, with an average value of 1,328 mm (sd = 165.6 mm). These conditions are considered suitable for agricultural production. In agreement with the RS_L data, we observed highest RS_{TPA} in Mato Grosso (1,507 mm, sd = 99.9 mm), followed by Tocantins (1,420 mm, sd = 132.6 mm), Rondônia (1,295 mm, sd = 160.0 mm), and Goiás (1,254 mm, sd = 99.9 mm). Notably, the spatial variability of precipitation followed the spatial distribution of natural vegetation, with savannas located in the drier southeastern regions and rainforests located in the wetter northwestern regions (Figure 3D). Highest precipitation was observed in the central northern region of Mato Grosso within the Serra do Cachimbo (Figure 3D). A similar rainfall distribution was observed by Arvor *et al.* (2014). The spatial standard deviations for RS_L and RS_{TPA} indicate regions of high variability in southeast Rondônia and north Tocantins, respectively (Supplementary Figure S2, C, and D).

3.1.3. Number of dry and wet days during the rainy season

RS_{NDD} ranged from 39 to 133 days across the study region, with an average of 69 days (sd = 14.8 days). The highest number of dry days were observed in the north and central eastern regions of Mato Grosso (Figure 3E). The state showed significant spatial and temporal RS_{NDD} variability (also see Supplementary Fig. S2A), with an average of 82 days (sd = 21.5 days). Highest average RS_{NDD} values observed in Mato Grosso may be explained by the state's highest RS_L (Figure 5). In contrast, fewer dry days were observed in the states of Rondônia, Goiás, and Tocantins, with average RS_{NDD} values of 72, 69, and 51 days (sd = 10.3; 9.6; 4.6 days), respectively. Highest RS_{NWD} values were observed in the northeast region (mainly in Tocantins) and decreased southwards (Figure 3F), which is consistent with the spatial variability of RS_{NDD}. This suggests that rainfall is well distributed during the growing season in Tocantins. Highest average RS_{NDD} was observed in Tocantins at 117 (sd = 8.2) days, followed by Mato Grosso (94 days, sd = 16.0 days), Rondônia (94 days, sd = 9.89 days), and Goiás (92 days, sd = 13.1 days).

3.1.4. Growing season onset and number of dry and wet days

Average GS_{START} across the region varied by 35 days, occurring from the beginning of October (277 DOY) to the beginning of November (312 DOY). The average GS_{START} across the study region was at the end of October (301 DOY, sd = 7.1). Earliest seasonal onsets occurred across central and northern regions of Mato Grosso, followed by Goiás, Tocantins, and Rondônia (Figure 4A). The mean seasonal onset in Mato Grosso occurred in mid-October (295 DOY, sd = 10.4 DOY), while that of Rondônia, Tocantins, and Goiás occurred at the end of October (300, 302, and 303 DOY, sd = 9.0; 4.1; and 4.8 DOY, respectively). Figure 5 illustrates the GS_{START} variability among the different states. The number of wet (GS_{NDD}) and dry days (GS_{NWD}) during the growing season were consistent with the number of wet and dry days during the rainy season (Figure 4C and D). The state of Tocantins had the highest number of wet days during the growing season (118 days, sd = 7.7 days), followed by Rondônia (94, sd = 9.9), Mato Grosso (93, sd = 16), and Goiás (90, sd = 12.6). We observed significant temporal variability in the number of wet and dry days, particularly in the states of Mato Grosso and Goiás (Supplementary Figure S3B, C), which is consistent with the rainy season characteristics.

3.2 Relationships between climatological variables

All climatological variables (RS_{START}, RS_{END}, RS_{L}, $RS_{TPA,}$ RS_{NDD}, $RS_{NWD,}$ $GS_{START,}$ $GS_{NDD,}$ $GS_{NDD,}$ and GS_{NWD}) were weakly (Spearman's rho < = 0.19 in absolute value) correlated with longitude. Similarly, only two rainy season variables (RS_{TPA} and RS_{END})

were weakly positively correlated with latitude (Spearman rho = 0.21, Figure 6). Interestingly, we observed no correlation between RS_{START} and RS_{END}, inferring different controlling physical processes on the begin and end dates of the rainy season (Spearman's rho = -0.02).

As expected, we identified a very strong correlations (Spearman's rho > 0.80 of absolute values) between RS_{START} and GS_{START}; RS_{NWD} and GS_{NWD}; and RS_{NDD} and GS_{NDD}. Strong correlations (Spearman's rho from 0.60 to 0.79 in absolute value) were also observed between RS_L and RS_{START}, GS_{START}, RS_{END}, and RS_{TPA}. The strong linear relationship between RS_L and RS_{START} is particularly crucial, since early detection of RS_{START} in a particular year and a particular location can help to predict the duration of the upcoming season. This estimation can thus adequately define which crops or crop varieties may be suitable for cultivation. As expected, we also identified a strong correlation between RS_{TPA} and RS_{NWD} and GS_{NWD} (Figure 6).

3.3. Effect of ENSO on rainfall and growing season characteristics

The effect of ENSO (El Niño, Neutral, La Niña) on rainfall and growing season characteristics in each state is shown in Table 2 and Figure 5. La Niña and El Niño were shown to influence RS_{START} only in Mato Grosso, in which the quartile distribution of La Niña and El Niño suggests to be different to that of Neutral years (Figure 5). In contrast, RS_{END} was not affected by ENSO, but the RS_{END} was highly variable among the different states (Table 2 and Figure 5). El Niño was shown to influence RS_L only in Mato Grosso and Tocantins (Table 2), as the RS_L quartile distribution of El Niño years suggest to be different from that of Neutral and La Niña years in both states (Figure 5). RS_{NDD} seems to be reduced during La Niña years throughout the entire region; however, we did not observe obvious state-specific impacts (Table 2). Figure 5 also shows the quartile difference for RS_{NDD} between La Niña, Neutral, and El Niño phases. We found La Niña to influence RS_{NWD} in Rondônia, and El Niño to influence RS_{NWD} in Tocantins (Table 2). We observed a positive increment for the interaction between La Niña and Rondônia and a negative increment for the interaction between El Niño and Tocantins. We identified a trend toward increasing wet days in Rondônia during La Niña years and a trend toward decreasing dry days in Tocantins during El Niño years (Table 2). RS_{TPA} in Mato Grosso tends to be positively affected by La Niña years, and RS_{TPA} in Rondônia and Tocantins tends to be positively affected by El Niño years (Table 2). Our findings suggest that while La Niña phases increase precipitation in Mato Grosso, El Niño phases increase precipitation in Rondônia and Tocantins.

The onset of the growing season was influenced by both La Niña and El Niño in Mato Grosso, while only La Niña was shown to influence the growing season onset in the remaining states (Table 2). GS_{NDD} was positively affected by La Niña in Rondônia and negatively influenced by El Niño in Tocantins (Table 2). GS_{NDD} was positively affected by La Niña in Mato Grosso and negatively influenced by El Niño in Tocantins (Table 2).

3.4. Water use dynamics and the crop sowing calendar

GS_{START} was affected by La Niña and El Niño in Mato Grosso (Table 2). We conducted crop model simulations to determine the beginning (average GS_{START} – standard deviation), mean optimal (average GS_{START}), and end (average GS_{START} + standard deviation) dates of the growth season for Neutral, La Niña, and El Niño years at each weather station in Mato Grosso.

In general, we found a broad range of sowing dates in Mato Grosso, which were suitable for the production of upland rice and a number of other crops across the study region (Figure 7). Within this sowing window (see sowing calendar in Figure 7), the sowing date with greatest water availability (mean optimal sowing date) corresponds to the mean value of GS_{START} (white checked circles in Figure 7). Upland rice does not experience water stress during the sensitive initial growth stage (the first 30 days after sowing) when it is sown at or very close to mean value of GS_{START}. For early sowing dates, we find that the mean accumulated precipitation in the first 15 and 30 days after sowing was consistently lower under early sowing dates relative to later and mean optimal sowing dates (Supplementary Figure S5 and S6). In addition, the mean PCEW (ratio of actual to potential transpiration, crop model output) in the first 30 days after sowing was consistently near 1 (no water stress) under later and mean optimal sowing dates relative to early sowing dates (Supplementary Figure S9 and S10).
We identified longer range in sowing periods during Neutral years (top panel, Figure 7) for most weather stations in Mato Grosso relative to El Niño (middle panel, Figure 7) and La Niña years (bottom panel, Figure 7). The mean optimal sowing date was generally delayed in La Niña years.

GS_{START} in Goiás, Tocantins, and Rondônia was affected only during La Niña years (Table 2). For these states, we conducted crop model simulations for Neutral, El Niño, and La Niña years to determine the start (average GS_{START} – standard deviation), mean optimal (average GS_{START}), and end (average GS_{START} + standard deviation) dates for each weather station. We identified a broad range of sowing dates for Goiás, Rondônia, and Tocantins, which are considered suitable for the production of upland rice and a number of other crops across the study region (Figure 8 and 9). On average, the sowing period was shorter and the mean optimal date was delayed during La Niña years (Figure 8 and 9) in Goiás. For all states, sowing earlier or later than the mean optimal sowing date leads to increased water stress; however, the season is still suitable for upland rice and other crop production across Central Brazil. Previous studies using crop model simulations showed that early sowing can increase the risk of drought for upland rice (Heinemann *et al.*, 2015), though this effect was only limited to some weather stations. Earlier sowing was also linked to lowest accumulated precipitation in the first 15 and 30 days after sowing (Supplementary Fig. S7 and S8). In addition, the mean PCEW (ratio of actual to potential transpiration, crop model output) in the first 30 days after sowing was consistently near 1 (no water stress) under later and mean optimal sowing dates relative to early sowing dates (Supplementary Figure S11, S12 and S13). Early soybean sowing in Central Brazil was also found to increase the risk of crop loss due to water deficits (Nóia Júnior and Sentelhas, 2019b).

4. Discussion

4.1. ENSO effects on rainy and cropping season length

Of the four states in Central Brazil, we observed the longest rainy seasons in Mato Grosso and Tocantins, with earlier rainfall onsets and later rainfall cessations. However, Tocantins showed greater suitability for crop production, as the number of dry days during the rainfall season was significantly lower than that of Mato Grosso. This result for Tocantins is in contrast to the weak positive correlation between rainy season duration and the number of dry days observed in all other states. Our results demonstrate that a negative ENSO phase (La Niña) significantly decreases the number of dry days in the rainy season and growing season across the entire region. La Niña was also found to delay the start of the growing season ($p < 0.05$). Tocantins experiences the most significant ENSO effects, particularly during warm ENSO phases (El Niño), leading to higher but infrequent rainfall events. El Niño phases also impact Mato Grosso, leading to slightly earlier rainfall onsets and a longer seasonal duration. In contrast, cold ENSO (La Niña) phases predominantly affect Rondônia, leading to an increased frequency of high total rainfall. As is expected, the cooler surface waters in the eastern Pacific during La Niña years cause a reduction in the number of dry days during the growing season compared to Neutral and El Niño years. The typical El Niño rainfall anomaly pattern is most evident over the northern/northeastern regions of South America, with drier conditions over southern/southeastern regions (Grimm, 2003; Andreoli *et al.*, 2017).

4.2. Implications of ENSO for crop production

Our results indicate that ENSO has no impact on the yield of primary crops sown at the end of October/beginning of November (which represents the main rainy season of crop production), but influences the yield of secondary crops sown after February, such as maize (also referred to as "safrinha"), as observed by Anderson et al. (2017) and Arvor et al. (2012). Double cropping—particularly soybean–maize rotations—is common in Mato Grosso, Rondônia, and regions of Goiás. Low secondary crop yield can be attributed to La Niña due to lowered soil water content. We found a reduction in the length of the sowing window by 23%, 22%, and 13% during La Niña years (Figure 7, 8, and 9) in Goiás, Tocantins, and Rondônia, respectively, relative to Neutral and El Niño years. In Mato Grosso, we observed an 18% decrease relative to

Neutral years. We also observed a delay in the mean optimal sowing date during La Niña years for all states and during El Niño years for Mato Grosso. A narrower sowing window and a delayed in the mean optimal sowing date is unlikely to be a limitation in regions with only a single cropping season. Sowing soybean in late October/start of November (which includes the estimated mean optimal sowing date (Figure 7 and 8)) would result in the sowing of the secondary crop in late February/early March. However, further delays in the sowing of the secondary crop would increase the risk of water deficits (Soler *et al.*, 2007a, b). From the results of this study, we can infer that a delay of 15 days, in addition to the duration of the sowing operation (2–4 weeks), would lead to the sowing of secondary crops after February, which increases the risk of a water deficit. For double cropping, we therefore recommend that different strategies be adopted by farmers for both La Niña (all states) and El Niño years (Mato Grosso), such as avoiding the sowing of secondary crops, selecting a secondary crop that is less susceptible to water deficits (e.g., sorghum instead of maize), or selecting shorter cycle genotypes for soybean and maize, particularly in Goiás. Our results are useful for improved decision making of farmers, governments, insurance companies, input industries, and other sectors involved in agriculture production.

The sowing dates identified in this study are based on rice model simulations. However, we believe the established sowing windows are transferable to other annual and drought tolerant crops, such as maize and soybean. The onset dates of the growing season obtained in this study (shown in Figure 7, 8, and 9) can be used to assist farmers and government agencies to develop adaptation strategies that will maximize productivity and reduce climate-induced risks to crop production. Our model simulations also indicate that earlier and later sowing dates are possible but less optimal relative to sowing at the long-term (1980–2013) average growing season start date compared to fixed earlier or later long-term (1980-2013) sowing date. Our findings also indicate that the length of the sowing period is not a limitation for single crop seasons. However, under crop rotation, early sowing in Central Brazil would have a negative impact on the primary crop yield (Figures 7–9) due to the increased risk of water deficits during the vegetative phase of crop growth. In contrast, late sowing will increase the risk of crop loss by water deficit during the grain filling phase of secondary crop growth. Importantly, we find no need to adjust the sowing windows for one crop season depending on ENSO conditions.

4.3. Limitations and future work

Here, we have used the best available data to address the question of whether ENSO has a significant impact on the rainy and growing season dynamics in central Brazil. While our findings are robust and generally complement with existing studies, several limitations become apparent. Notably, the quality and geographical distribution of the weather stations is not perfect and can introduce errors to the estimation of the rainy and growing season characteristics and their interpolation across the region. We deem errors introduced by gaps in the weather station time series small or negligible, since gaps tend to be randomly spread across the time series (rather than occurring in continuous period), are in general less than 20% of the total length of the time series, and are filled using reliable alternative sources (ANA and CPC). Likewise, the distribution of weather stations is not uniform, and likely to affect spatial interpolation results. However, we note that IDW interpolations are performed here as a way of assessing spatial trends in the characteristics of the growing season, rather than predicting such characteristics in specific locations.. These trends are consistent with prior knowledge and literature, and are found to adequately represent the study region, which gives confidence that the distribution of weather stations is unlikely to hinder our conclusions. Future work could extend our analysis to be performed with gridded datasets (Xavier et al., 2016; Battisti et al., 2019) to verify the robustness of the spatial trends found here. Similarly, future work can extend our analysis to other crops, both confirming that findings for rice are indeed extensible to other annual crops but also creating reliable crop calendars for crops that are less likely to be represented by rice (e.g. cassava, potato, wheat, barley). Finally, we believe our work can also be extended to other cropping regions of Brazil, and, in the future connected to farmer advisory systems for supporting decision making on planting dates, if a denser and more evenly distributed network of weather stations was established. The latter can be done through linking our modeling approach to existing weather, sub-seasonal and/or seasonal forecasting systems (Chou et al., 2000; Coelho et al., 2006; Martins et al., 2018).

Acknowledgments

JR-V acknowledges support from the CGIAR Research Programme on Climate Change, Agriculture and Food Security (CCAFS) under the Agroclimas (phase 1 and 2) project. CCAFS is conducted with support from the CGIAR Trust Fund Donors and through bilateral funding agreements; for details, please visit https://ccafs.cgiar.org/donors. The views expressed in this paper do not reflect the official opinions of these organizations. JR-V is also supported by the Climate Services for Resilient Development (CSRD)-United States Agency for International Development (USAID) Award#: AID-BFS-G-11-00002-10 towards the CGIAR Fund (MTO 069018). CSRD (http://www.cs4rd.org/) brings together public and private organizations and agencies committed to realizing the potential to enhance climate resilience and climate-smart policies and practices throughout the world, particularly in developing countries. AB Heinemann acknowledges support from “Fundação de Amparo à Pesquisa do Estado de Goiás” (FAPEG - PRONEM/FAPEG/CNPq) and “Conselho Nacional de Desenvolvimento Científico e Tecnológico” (CNPq – Edital Universal – Processo - 408025/2018-2)

References

Abrahão, G.M. and Costa, M.H. (2018) Evolution of rain and photoperiod limitations on the soybean growing season in Brazil: The rise (and possible fall) of double-cropping systems. *Agricultural and Forest Meteorology*, 256–257, 32-45. https://doi.org/10.1016/j.agrformet.2018.02.031

Alvares, C.A., Stape, J.L., Sentelhas, P.C., Gonçalves, J.L.M. and Sparovek, G. (2013) Koppen's climate classification map for Brazil. *Meteorologische Zeitschrift*, 22, 711–728. https://doi.org/10.1127/0941-2948/2013/0507

Anderson W., Seager R., Walter, B. and Cane, M. (2017) Crop production variability in North and South America forced by life-cycles of the El Niño Southern Oscillation. *Agricultural and Forest Meteorology*, 239, 151-165. https://doi.org/10.1016/j.agrformet.2017.03.008

Andreoli, R.V., Oliveira, S.S., Kayano, M.T., Viegas, J., Souza, R.A. and Candido, L.A. (2017) The influence of different El Niño types on the South American rainfall. *International Journal of Climatology*, 37, 1374-1390. https://doi.org/10.1002/joc.4783

Araya, A., Keesstra, S.D. and Stroosnijder, L. (2010) A new agro-climatic classification for crop suitability zoning in northern semi-arid Ethiopia. *Agricultural and Forest Meteorology*, 150, 1057–1064. https://doi.org/10.1016/j.agrformet.2010.04.003

Arvor, D., Meirelles, M., Dubreuil, V., Bégué, A. and Shimabukuro, Y.E. (2012) Analyzing the agricultural transition in Mato Grosso, Brazil, using satellite-derived indices *Applied Geography*, 32, 702-713. https://doi.org/10.1016/j.apgeog.2011.08.007

Arvor, D., Dubreuil, V., Ronchail, J., Simões, M. and Funatsu, B.M. (2014) Spatial patterns of rainfall regimes related to levels of double cropping agriculture systems in Mato Grosso (Brazil). *International Journal of Climatology*, 34, 2622–2633. http://dx.doi.org/10.1002/joc. 3863

Battisti, R., Bender, F.D., Sentelhas, P.C. (2018a). Assessment of different gridded weather data for soybean yield simulations in Brazil. Theor. Appl. Climatol. 1–11. https://doi. org/10.1007/s00704-018-2383-y.

Battisti, R., Sentelhas, P.C., Pascoalino, J.A.L., Sako, H., de Sá Dantas, J.P., Moraes, M.F. (2018b). Soybean yield gap in the areas of yield contest in Brazil. Int. J. Plant Prod. https://doi.org/10.1007/s42106-018-0016-0.

Battisti, R., Bender, F. D., and Sentelhas, P. C. (2019). Assessment of different gridded weather data for soybean yield simulations in Brazil. *Theor. Appl. Climatol.* 135, 237–247. doi:10.1007/s00704-018-2383-y.

Bhuvaneswari, K., Geethalakshmi, V., Lakshmanan, A., Srinivasan, R. and Sekhar, U.N. (2013) The impact of El Niño/Southern oscillation on hydrology and rice productivity in the Cauvery Basin, India: application of the soil and water assessment tool. *Weather and Climate Extremes*, 2, 39-47. https://doi.org/10.1016/j.wace.2013.10.003

Carvalho, L.M.V., Jones, C. and Liebmann, B. (2004) The South Atlantic convergence zone: intensity, form, persistence, and relationships with intraseasonal to interannual activity and extreme rainfall. *Journal of Climate*, 17, 88–108. https://doi.org/10.1175/1520-0442(2004)017<0088:TSACZI>2.0.CO;2

Carvalho, L.M.V, Jones, C., Silva, A.E., Liebmann, B. and Silva Dias, P.L. (2011) The South American Monsoon System and the 1970s climate transition. *International Journal of Climatology*, 31, 1248–1256. https://doi.org/10.1002/joc.2147

Coelho, C.A.S., Uvo, C.B. and Ambrizzi, T. (2002) Exploring the impacts of the tropical Pacific SST on the precipitation patterns over South America during ENSO periods. Theoretical and Applied Climatology, 71, 185–197. https://doi.org/10.1007/s007040200004

CONAB (2018) Acompanhamento da safra brasileira de grãos: safra 2017/18. https://www.conab.gov.br

Debortoli, N.S., Dubreuil, V., Funatsu, B., Delahaye, F., Oliveira, C.H., Rodrigues-Filho, S., Saito, C.H. and Fetter, R. (2015) Rainfall patterns in the Southern Amazon: a chronological perspective (1971–2010). *Climatic Change*, 132, 251–264. https://doi.org/10.1007/s10584-015-1415-1

Delerce, S., Dorado, H., Grillon, A., Rebolledo, M.C., Prager, S.D., Patiño, V.H., Varón, G.G. and Jiménez, D. (2016) Assessing weather-yield relationships in rice at local scale using data mining approaches. *PLoS One*, 11, e0161620. https://doi.org/10.1371/journal.pone.0161620

Dunning, C.M., Black, E.C.L. and Allan, R.P. (2016) The onset and cessation of seasonal rainfall over Africa. *JGR Atmospheres*, 121, 11-405–11-424. https://doi.org/10.1002/2016JD025428

Fraisse, C.W., Cabrera, V.E., Breuer, N.E., Baez, J., Quispe, J. and Matos, E. (2008) El Niño—Southern oscillation influences on soybean yields in eastern Paraguay. *International Journal of Climatology*, 28, 1399–1407. https://doi.org/10.1002/joc.1641

Funatsu, B., Dubreuil, V., Claud, C., Arvor, D. and Gan, M. (2012) Convective activity in Mato Grosso State (Brazil) from microwave satellite observations: comparisons between AMSU and TRMM datasets. *Journal of Geophysical Research*, 177, 1–16.

Gan, M.A., Kousky, V.E. and Ropelewski, C.F. (2004) The South America monsoon circulation and its relationship to rainfall over West-Central Brazil. *Journal of Climate*, 17, 47–66. https://doi.org/10.1175/1520-0442(2004)017<0047:TSAMCA>2.0.CO;2

Gelcer, E., Fraisse, C., Dzotsi, K., Hu, Z., Mendes, R. and Zotarelli, L. (2013) Effects of El Niño Southern oscillation on the space–time variability of agricultural reference index for drought in midlatitudes. *Agricultural and Forest Meteorology*, 174–175, 110-128. https://doi.org/10.1016/j.agrformet.2013.02.006

Gräler B., Pebesma E, and Heuvelink G. (2016). Spatio-Temporal Interpolation using gstat. *The R Journal* 8(1), 204-218.

Grimm, A.M. (2003) The El Niño impact on the summer monsoon in Brazil: regional processes versus remote influences. *Journal of Climate*, 16, 263–280. https://doi.org/10.1175/1520-0442(2003)016<0263:TENIOT>2.0.CO;2

Grimm, A.M. and Tedeschi, R.G. (2009) ENSO and extreme rainfall events in South America. *Journal of Climate*, 22, 1589–1609. https://doi.org/10.1175/2008JCLI2429.1

Grimm, A.M. and Pscheidt, I. (2001) Atmospheric patterns associated with extreme rainfall events in the spring during El Niño, La Niña and neutral years in southern Brazil (in Portuguese). In: Proceedings. Ninth Congress of the Latin-American and Iberian Federation of Meteorological Societies and Eighth Argentinean Congress of Meteorology, Buenos Aires, Argentina.

Heinemann, A.B., Ramirez-Villegas, J., Rebolledo, M.C., Costa Neto, G.M.F. and Castro, A.P. (2019) Upland rice breeding led to increased drought sensitivity in Brazil. *Field Crops Research*, 231, 57–67. https://doi.org/10.1016/j.fcr.2018.11.009

Heinemann, A.B. Barrios-Perez, C., Ramirez-Villegas, J., Arango-Londoño, D., Bonilla-Findji, O., Medeiros, J.C. and Jarvis, A. (2015) Variation and impact of drought-stress patterns across upland rice target population of environments in Brazil. *Journal of Experimental Botany*, 66, 3625–3638. https://doi.org/10.1093/jxb/erv126

Hijmans, R. J. & van Etten J. (2012). raster: Geographic analysis and modeling with raster data. R package version 2.0-12. http://CRAN.R-project.org/package=raster

Iizumi, T., Luo, J-J., Challinor, A.J., Sakurai, G., Yokozawa, M., Sakuma, H., Brown, M.E. and Yamagata, T. (2014) Impacts of El Niño Southern oscillation on the global yields of major crops. *Nature Communications*, 5, 3712. https://doi.org/10.1038/ncomms4712

Li, T., Angeles, O., Marcaida, M., Manalo, E., Manalili, M.P., Radanielson, A. and Mohanty, S. (2017) From ORYZA 2000 to ORYZA (v3): An improved simulation model for rice in drought and nitrogen-deficient environments. *Agricultural and Forest Meteorology*, 237–238, 246–256. https://doi.org/10.1016/j.agrformet.2017.02.025

Li, W. and Fu, R. (2006) Influence of cold air intrusions on the Wet Season Onset over Amazonia. *Journal of Climate*, 19, 257–275. https://doi.org/10.1175/JCLI3614.1

Liebmann, B. and Marengo, J. (2001) Interannual variability of the rainy season and rainfall in the Brazilian Amazon Basin. *Journal of Climate*, 14, 4308-4318. https://doi.org/10.1175/1520-0442(2001)014<4308:IVOTRS>2.0.CO;2

Liebmann, B., Camargo, S.J., Seth, A., Marengo, J.A., Carvalho, L.M.V., Allured, D., Fu, R. and Vera, C.S. (2007) Onset and end of the rainy season in South America in observations and the ECHAM 4.5 Atmospheric General Circulation Model. *American Meteorological Society*, 20, 2037- 2050. https://doi.org/10.1175/JCLI4122.1

Liebmann, B., Bladé, I., Kiladis, G.N., Carvalho, L.M., Senay, G.B., Allured, D., Leroux, S. and Funk, C. (2012) Seasonality of African precipitation from 1996 to 2009. *Journal of Climate*, 25, 4304–4322. https://doi.org/10.1175/JCLI-D-11-00157.1

Liu, W.T. and Juárez, R. (2001) ENSO drought onset prediction in northeast Brazil using NDVI. *International Journal of Remote Sensing*, 17, 3483-3501. https://doi.org/10.1080/01431160010006430

Liu, Y., Yang, X., Wang, E. and Xue, C. (2014). Climate and crop yields impacted by ENSO episodes on the North China Plain: 1956–2006. *Regional Environmental Change*, 14, 49–59. https://doi.org/10.1007/s10113-013-0455-1

Marengo, J.A. (2006) On the hydrological cycle of the Amazon Basin: a historical review and current state-of-the-art. *Revista Brasileira de Meteorologia*, 21, 1–19.

Marengo, J.A., Liebmann, B., Kousky, V.E., Filizola, N.P. and Wainer, I.C. (2001) Onset and end of the rainy season in the Brazilian Amazon basin. *Journal of Climate*, 14, 833–852. https://doi.org/10.1175/1520-0442(2001)014<0833:OAEOTR>2.0.CO;2

Marteau, R., Sultan, B., Moron, V., Alhassane, A., Baron, C. and Traoré, S.B. (2011) The onset of the rainy season and farmers' sowing strategy for pearl millet cultivation in Southwest Niger. *Agricultural and Forest Meteorology*, 151, 1356–1369. https://doi.org/10.1016/j.agrformet.2011.05.018

Mathugama, S.C. and Peiris, T.S.G. (2011) Critical evaluation of dry spell research. *International Journal of Basic & Applied Sciences IJBAS-IJENS*, 11, 153-160.

Mishra, A., Hansen, J.W., Dingkuhn, M., Baron, C., Traoré, S.B., Ndiaye, O. and Ward, M.N. (2008) Sorghum yield prediction from seasonal rainfall forecasts in Burkina Faso. *Agricultural and Forest Meteorology*, 148, 1798–1814. https://doi.org/10.1016/j.agrformet.2008.06.007

Moura, M.M., dos Santos, A.R., Pezzopane, J.E.M., Alexandre, R.S., da Silva, S.F., Pimentel, S.M., de Andrade, M.S.S., Silva, F.G.R., Branco, E.R.F., Moreira, T.R., da Silva, R.G., de Carvalho, J.R., 2019. Relation of El Niño and La Niña phenomena to precipitation, evapotranspiration and temperature in the Amazon basin. Sci. Total Environ. 651, 1639–1651. https://doi.org/10.1016/j.scitotenv.2018.09.242

Ngetich, K.F., Mucheru-Muna, M., Mugwe, J.N., Shisanya, C.A., Diels, J. and Mugendi, D.N. (2014) Length of growing season, rainfall temporal distribution, onset and cessation dates in the Kenyan highlands. *Agricultural and Forest Meteorology*, 188, 24–32. https://doi.org/10.1016/j.agrformet.2013.12.011

NOAA. 2019. Historical ENSO episodes (1950–present): Cold and warm episodes by season. National Weather Service, Climate Prediction Center. Available at: http://www.cpc.ncep.noaa.gov/products/analysis_monitoring/ensostuff/ensoyears_ERSSTv3b.shtml.

Nóia Júnior, R.S.; Sentelhas, P.C. 2019a. Soybean-maize off-season double crop system in Brazil as affected by El Niño Southern Oscillation phases, Agricultural Systems, 173: 254-267, https://doi.org/10.1016/j.agsy.2019.03.012.

Nóia Júnior, R.S.; Sentelhas, P.C. 2019b. Soybean-maize succession in Brazil: impacts of sowing dates on climate variability, yields and economic profitability Eur. J. Agron., 103: 140-151, 10.1016/j.eja.2018.12.008

Odekunle, T.O. (2004) Rainfall and the length of the growing season in Nigeria. *International Journal of Climatology*, 24, 467–479. https://doi.org/10.1002/joc.1012

Oguntunde, P.G., Lischeid, G., Abiodunc, B.J. and Dietrich, O. (2014) Analysis of spatial and temporal patterns in onset, cessation and length of growing season in Nigeria. *Agricultural and Forest Meteorology* 194: 77–87. https://doi.org/10.1016/j.agrformet.2014.03.017

Paeth, H., Capo-Chichi, A. and Endlicher, W. (2008) Climate change and food security in tropical West Africa -A dynamic-statistical modelling approach. *Erdkunde* 62, 101–115.

PBMC Painel Brasileiro de Mudanças Climáticas. (2014) *Impactos, vulnerabilidades e adaptação às mudanças climáticas*: primeiro relatório de avaliação nacional. COPPE. Universidade Federal do Rio de Janeiro, Rio de Janeiro, RJ, Brasil, (http://www.pbmc.coppe.ufrj.br/pt/publicacoes/relatorios-pbmc/item/impactos-vulnerabilidades-e-adaptacao-volume-2-completo)

Penalba, O.C., Rivera, J.A., 2016. Precipitation response to El Niño/La Niña events in southern South America – emphasis in regional drought occurrences. Adv. Geosci. 42, 1–14. https://doi.org/10.5194/adgeo-42-1-2016.

Ramirez-Villegas, J. and Challinor, A. (2012) Assessing relevant climate data for agricultural applications. *Agricultural and Forest Meteorology*, 161, 26–45. https://doi.org/10.1016/j.agrformet.2012.03.015

Ramirez-Villegas, J., Heinemann, A.B., Castro, A.P., Breseghello, F., Navarro-Racines, C., Li, T., Rebolledo, M.C. and Challinor, A.J. (2018) Breeding implications of drought stress under future climate for upland rice in Brazil. *Global Change Biology*, 24, 2035–2050. https://doi.org/10.1111/gcb.14071

Richardson CW, Wright DA. (1984). WGEN: a model for generating daily weather variables. Washington, DC: US Department of Agriculture.

Rippke, U., Ramirez-Villegas, J., Jarvis, A., Vermeulen, S.J., Parker, L., Mer, F., Diekkrüger, B., Challinor, A.J. and Howden, M. (2016) Timescales of transformational climate change adaptation in sub-Saharan African agriculture. *Nature Climate Changes*, 6, 605–609. https://doi.org/10.1038/nclimate2947

Rodrigues, R.R., Haarsma, R.J., Campos, E.D. and Ambrizzi, T. (2011) The impacts of inter--El Niño variability on the tropical Atlantic and Northeast Brazil Climate. *Journal of Climate*, 24, 3402-3422. https://doi.org/10.1175/2011JCLI3983.1

Simelton, E. (2011) Food self-sufficiency and natural hazards in China. *Food Security*, 3, 35–52. https://doi.org/10.1007/s12571-011-0114-7

Soler, C.M.T., Hoogenboom, G., Sentelhas, P.C., Duarte, A.P., 2007a. Impact of water stress on maize grown off-season in a subtropical environment. J. Agron. Crop Sci. 193, 247–261. https://doi.org/10.1111/j.1439-037X.2007.00265.x.

Soler, C.M.T., Sentelhas, P.C., Hoogenboom, G., 2007b. Application of the CSM-CERES- Maize model for planting date evaluation and yield forecasting for maize grown off- season in a subtropical environment. Eur. J. Agron. 27, 165–177. https://doi.org/10. 1016/j.eja.2007.03.002.

Van Wart, J., Grassini, P., Yang, H., Claessens, L., Jarvis, A. and Cassman, K.G. (2015) Creating long-term weather data from thin air for crop simulation modeling. *Agricultural and Forest Meteorology*, 209–210, 49–58. https://doi.org/10.1016/j.agrformet.2015.02.020

Verburg, R., Rodrigues Filho, S., Lindoso, D.P., Debortoli, N., Litre, G. and Bursztyn, M. (2014a) The impact of commodity price and conservation policy scenarios on deforestation and agricultural land use in a frontier area within the Amazon. *Land Use Policy* 37, 14–26. https://doi.org/10.1016/j.landusepol.2012.10.003

Verburg, R., Rodrigues Filho, S., Debortoli, N., Lindoso, D.P., Nesheim, I. and Bursztyn, M. (2014b) Evaluating sustainability options in an agricultural frontier of the Amazon using multi-criteria analysis. *Land Use Policy* 37, 27–39. https://doi.org/10.1016/j.landusepol.2012.12.005

Xavier, A. C., King, C. W., and Scanlon, B. R. (2016). Daily gridded meteorological variables in Brazil (1980-2013). *Int. J. Climatol.* 36, 2644–2659. doi:10.1002/joc.4518.

Zabel, F., Putzenlechner, B. and Mauser, W. (2014) Global agricultural land resources – A high resolution suitability evaluation and its perspectives until 2100 under climate change conditions. *PLoS One*, 9, e107522. https://doi.org/10.1371/journal.pone.0107522

Table 1. Weather station identification, latitude, longitude, altitude and average annual rainfall during the period 1980–2013 (33 years).

ID	State	County name	Lat	Long	Altitude (m)	Rainfall (mm year^{-1})
1		Parauna	-17.51	-50.49	721	1448
2		Santo Antônio de Goiás	-16.47	-49.28	860	1528
3		Goiânia	-16.59	-49.27	749	1438
4		Aragarcas	-15.9	-52.23	310	1458
5		Formosa	-15.53	-47.33	916	1336
6		Ipameri	-17.72	-48.17	764	1412
7		Pirenopolis	-15.85	-48.97	770	1609
8		Posse	-14.1	-46.37	811	1349
9		Rio Verde	-17.8	-50.92	715	1419
10		Faina	-15.43	-50.37	360	1517
11		Luziania	-16.26	-47.97	930	1331
12		Porangatu	-13.43	-49.13	396	1522
13		Goiás	-15.94	-50.14	496	1667
14	Goiás	Caiaponia	-16.97	-51.82	692	1490
15		Monte Alegre de Goiás	-13.25	-46.89	557	1280
16		Morrinhos	-17.7	-49.11	771	1529
17		Quirinopolis	-18.6	-50.4	541	1486
18		Bom Jesus de Goiás	-18.07	-50.18	619	1298
19		Catalao	-18.05	-47.38	835	1355
20		Cristalina	-17.11	-47.31	1189	1599
21		Jatai	-17.88	-51.72	696	1517
22		Anapolis	-16.3	-48.91	1017	1502
23		Aruana	-14.9	-51.00	250	1512
24		Caldas Novas	-17.71	-48.61	686	1488
25		Itumbiara	-18.41	-49.3	448	1290
26		Brazabrantes	-16.42	-49.38	761	1514
27		Planaltina	-15	-47	944	1291
28		Canarana	-13.47	-52.27	420	1658
29		Cuiaba	-14.4	-56.45	176	2019
30		Diamantino	-12.29	-55.29	269	1879
31		Matupa	-10.25	-54.92	280	2025
32	Mato Grosso	Nova Xavantina	-14.7	-52.35	275	1316
33		Alta Floresta	-10.07	-56.75	283	2042
34		Aripuana	-10.15	-59.45	105	1722
35		Rondonopolis	-16.45	-54.57	227	1555
36		Santo Antônio do Leverger	-15.78	-56.07	141	1671
37		Ji-Parana	-10.88	-61.97	170	1691

38	Rondônia	Porto Velho	-8.76	-63.91	85	1909
39		Ariquemes	-9.93	-62.96	142	1325
40		Cacoal	-11.48	-61.38	200	1358
41		Guajara-Mirim	-10.79	-65.28	128	1331
42		Machadinho D' Oeste	-9.4	-62.02	102	1416
43		Vilhena	-12.77	-60.09	600	1699
44	Tocantins	Araguaina	-7.2	-48.2	227	1654
45		Palmas	-10.19	-48.3	230	1737
46		Gurupi	-11.75	-49.05	287	1311
47		Peixe	-12.02	-48.35	240	1473
48		Taguatinga	-12.4	-46.42	599	1699
49		Pedro Afonso	-8.96	-48.18	201	1676
50		Porto Nacional	-10.71	-48.41	212	1655

Table 2. Variance characteristics of the applied statistical methods based on Bayesian information criterion (BIC).

Explanatory Variables	Dependent Variables								
	Rainfall Season (RS)						Growing Season (GS)		
	START[1]	END[1]	L[1]	NDD[1]	NWD[1]	TPA[2]	START[1]	NDD[1]	NWD[1]
ENSO	Mean Increment (β coefficient)								
LaNina	0.009	-0.014	-0.023	-0.062**	-0.003	-38.543	0.01**	-0.085***	-0.023
Neutral	(base)	(base)	(base)	(base)	(base)	(base)	(base)	(base)	(base)
ElNino	0.007	-0.009	-0.018	-0.023	-0.006	31.221	0.007	-0.029	-0.023
STATE									
GO	(base)	(base)	(base)	(base)	(base)	(base)	(base)	(base)	(base)
MT	0.003	0.114***	0.059***	0.123**	-0.063	158***	-0.002	0.199***	-0.047
RO	0.009	0.069***	0.012	0.057	0.006	51.029	-0.005	0.103	0.066
TO	0.004	0.126***	0.066**	-0.576***	0.173***	174***	-0.002	-0.556***	0.227***
ENSO*STATE									
LaNina*GO	(base)	(base)	(base)	(base)	(base)	(base)	(base)	(base)	(base)
LaNina*MT	-0.019*	-0.028	0.017	-0.017	0.046	41.799	0.02**	-0.034	0.065
LaNina*RO	-0.016	0.000	0.034	-0.101	0.120**	101*	-0.02	-0.078	0.110**
LaNina*TO	0.003	0.002	0.002	0.118	-0.028	16.861	0.003	0.162**	-0.059
Neutral*GO	(base)	(base)	(base)	(base)	(base)	(base)	(base)	(base)	(base)
Neutral*MT	(base)	(base)	(base)	(base)	(base)	(base)	(base)	(base)	(base)
Neutral*RO	(base)	(base)	(base)	(base)	(base)	(base)	(base)	(base)	(base)
Neutral*TO	(base)	(base)	(base)	(base)	(base)	(base)	(base)	(base)	(base)
ElNino*GO	(base)	(base)	(base)	(base)	(base)	(base)	(base)	(base)	(base)
ElNino*MT	-0.023**	0	0.040*	0.053	0.029	-2.293	-0.017*	0.009	0.055
ElNino*RO	0.000	-0.001	0.007	0.018	-0.01	111**	0.002	0.011	-0.014
ElNino*TO	0.012	-0.043	-0.052*	0.086	-0.098**	126**	-0.002	0.164**	-0.081*
Constant	6.096***	3.709***	3.655***	2.177***	2.681***	1253***	6.5***	128***	2.82***

[1] and [2] indicate the best fitted model:
[1]is the Negative Binomial Regression Model for Panel Data with Random Intercept Effect and
[2] is the Longitudinal linear regression model for panel data with random intercept effect.
base - means the reference effect.
* level of statistical significance: *** p < 0.01, ** p < 0.05 and * p < 0.1;
START: onset, day of year;
END: cessation, day of year;
L: length, number of days;
NDD: number of dry days;
NWD: number of wet days;
TPA: total amount of precipitation, in mm.

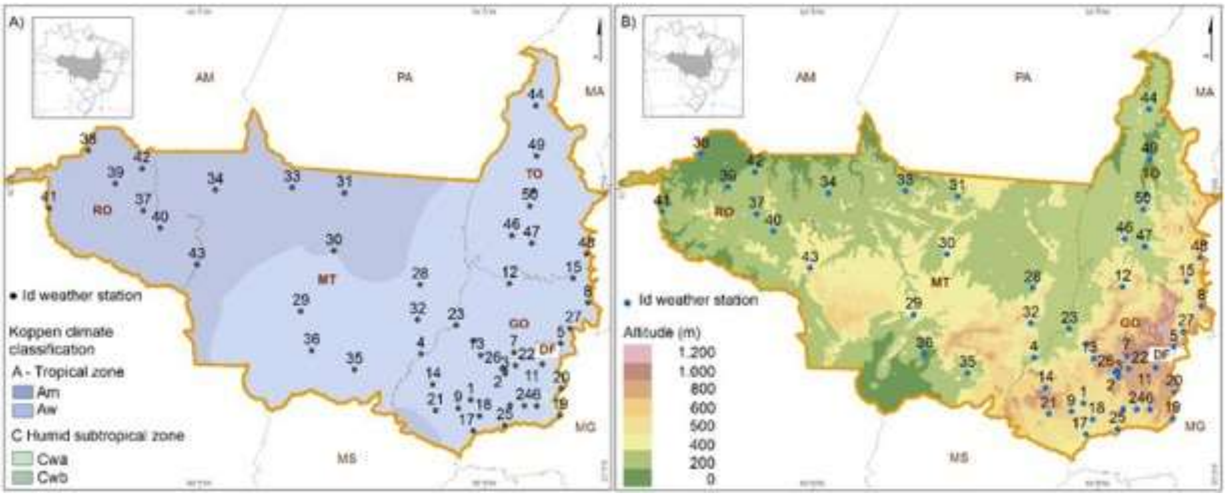

Figure 1. Distribution of weather stations (circles) across the study region overlaid on geographical maps of A) the Koppen's climate classification, and B) altitude. The numbers represent weather station identifiers shown in Table 1. The definition of each climate classification are as follows: 1) Am: < 60 mm rainfall (2.4 in) during the driest month (which typically occurs at or soon after the "winter" solstice south of the equator) and at least 100−(total annual precipitation (mm)/25); 2) Aw: a pronounced dry season, with < 60 mm (2.4 in) precipitation during the driest month and less than 100−(total annual precipitation (mm)/25); 3) Cwa: the precipitation of the driest month (in winter) is less than one-tenth of the precipitation in the wettest month (in summer), and temperatures are ≥ 22 °C in the warmest month; 4) Cwb: precipitation in the driest month (in winter) is less than one-tenth of the precipitation in the wettest month (in summer), the temperatures of the four warmest months are ≥ 10 °C, and the temperature of the warmest month is < 22 °C.

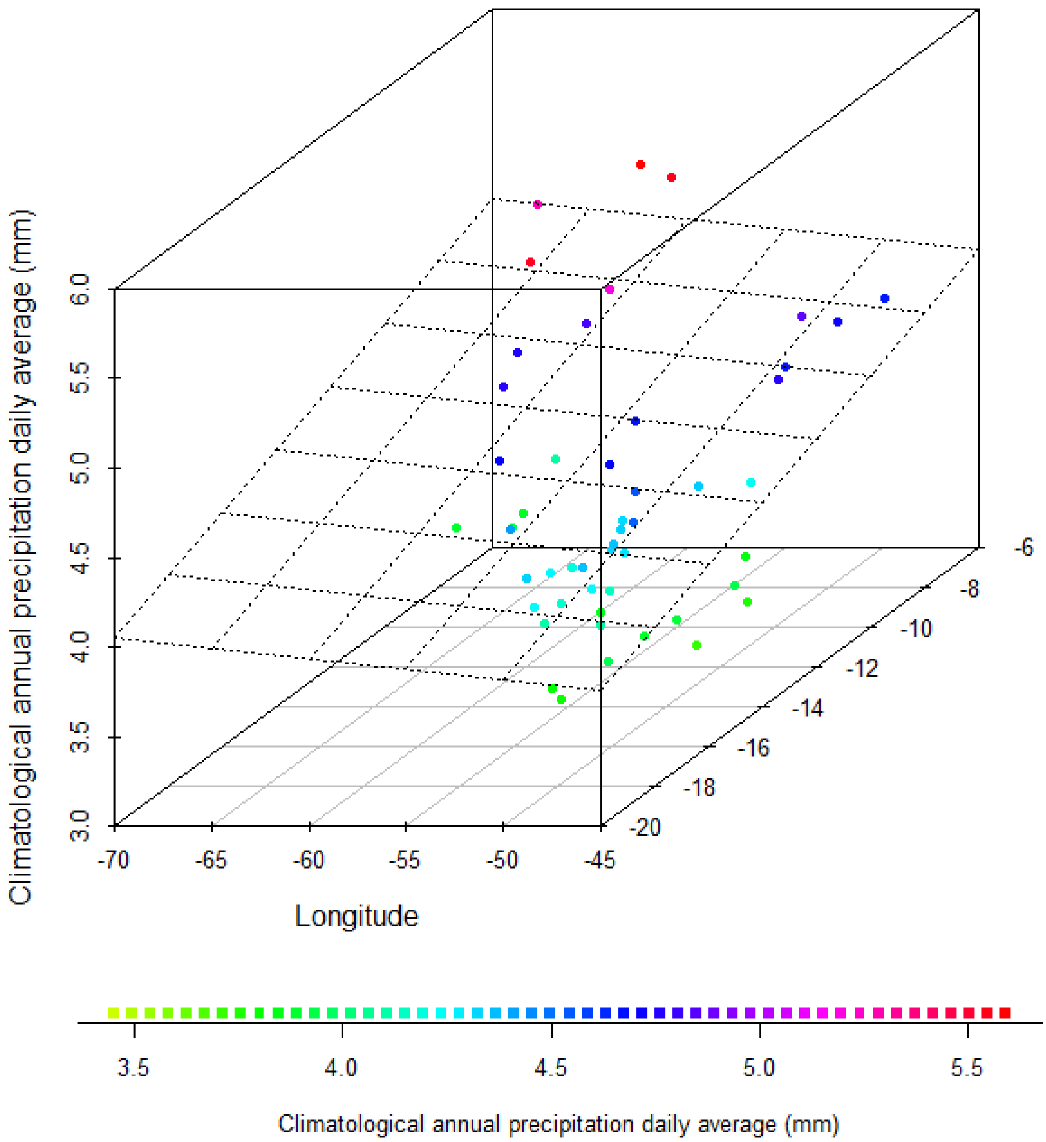

Figure 2. Spatial distribution of climatological annual average daily precipitation (R, from Equation 1) of the 50 weather stations. The geographical distribution of the weather stations is shown in Figure 1.

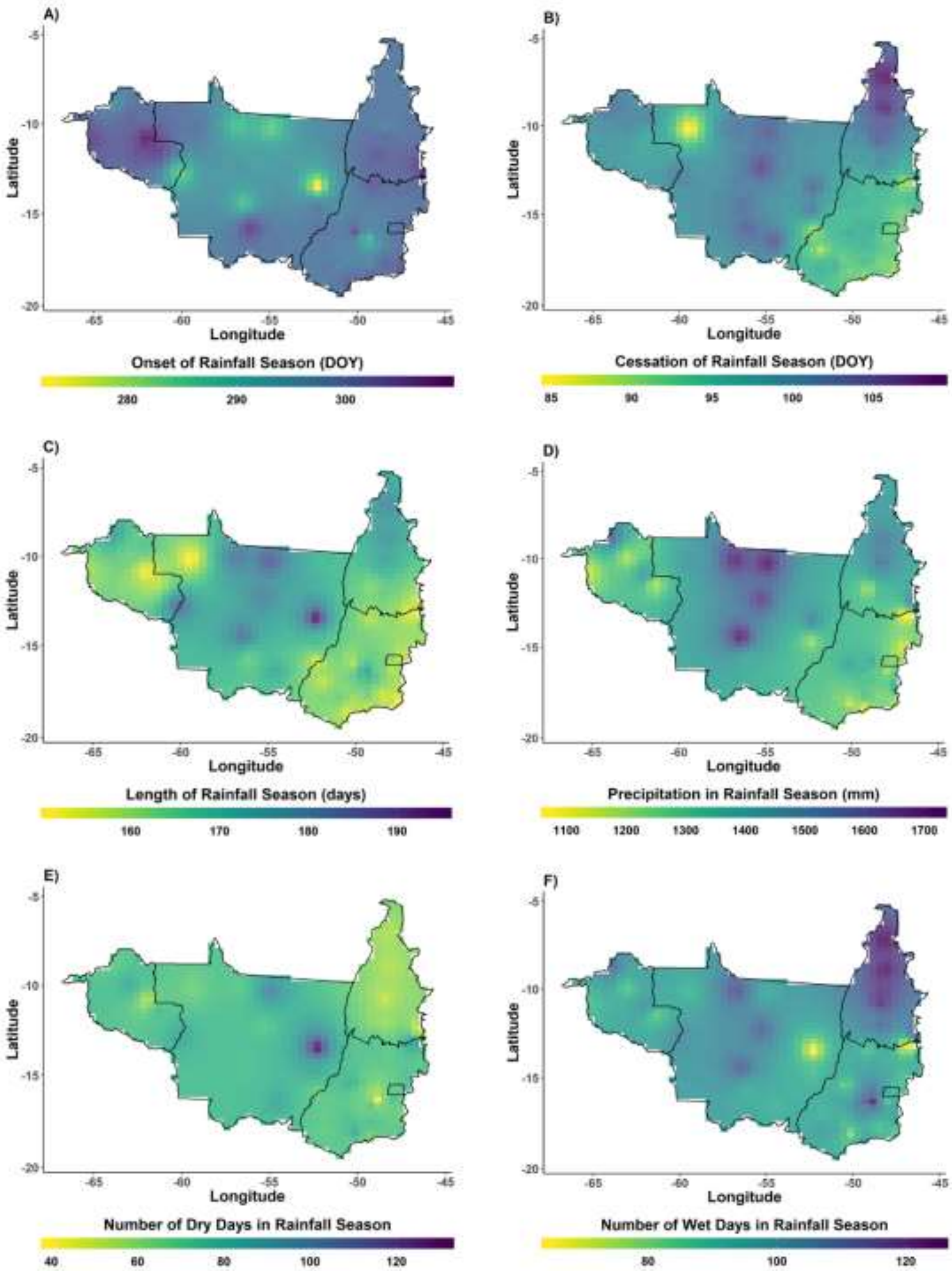

Figure 3. Spatial variability of averaged rainy season variables, including (A) rainy season onset (RS_{START} in DOY – day of year); (B) rainy season cessation (RS_{END} in DOY); (C) rainy season length (RS_{L} in days); (D) total precipitation throughout the rainy season (RS_{TPA} in mm); (E) the number of dry days during the rainy season (RS_{NDD} in days); and (F) the number of wet days during the rainy season (RS_{NWD} in days).

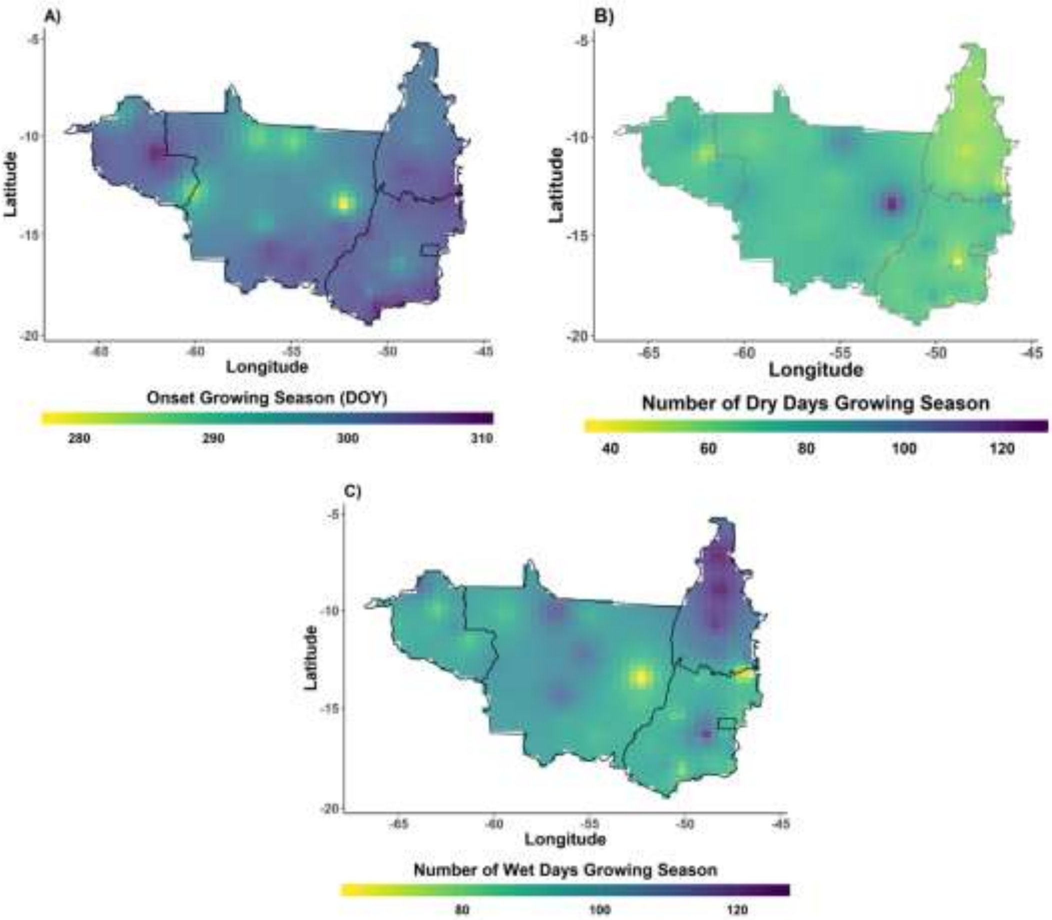

Figure 4. Spatial variability of averaged growing season climate variables, including (A) growing season onset (GS_{START} in DOY - day of year); (B) the number of wet days during the growing season (GS_{NWD}); and (C) the number of dry days during the growing season (GS_{NDD}).

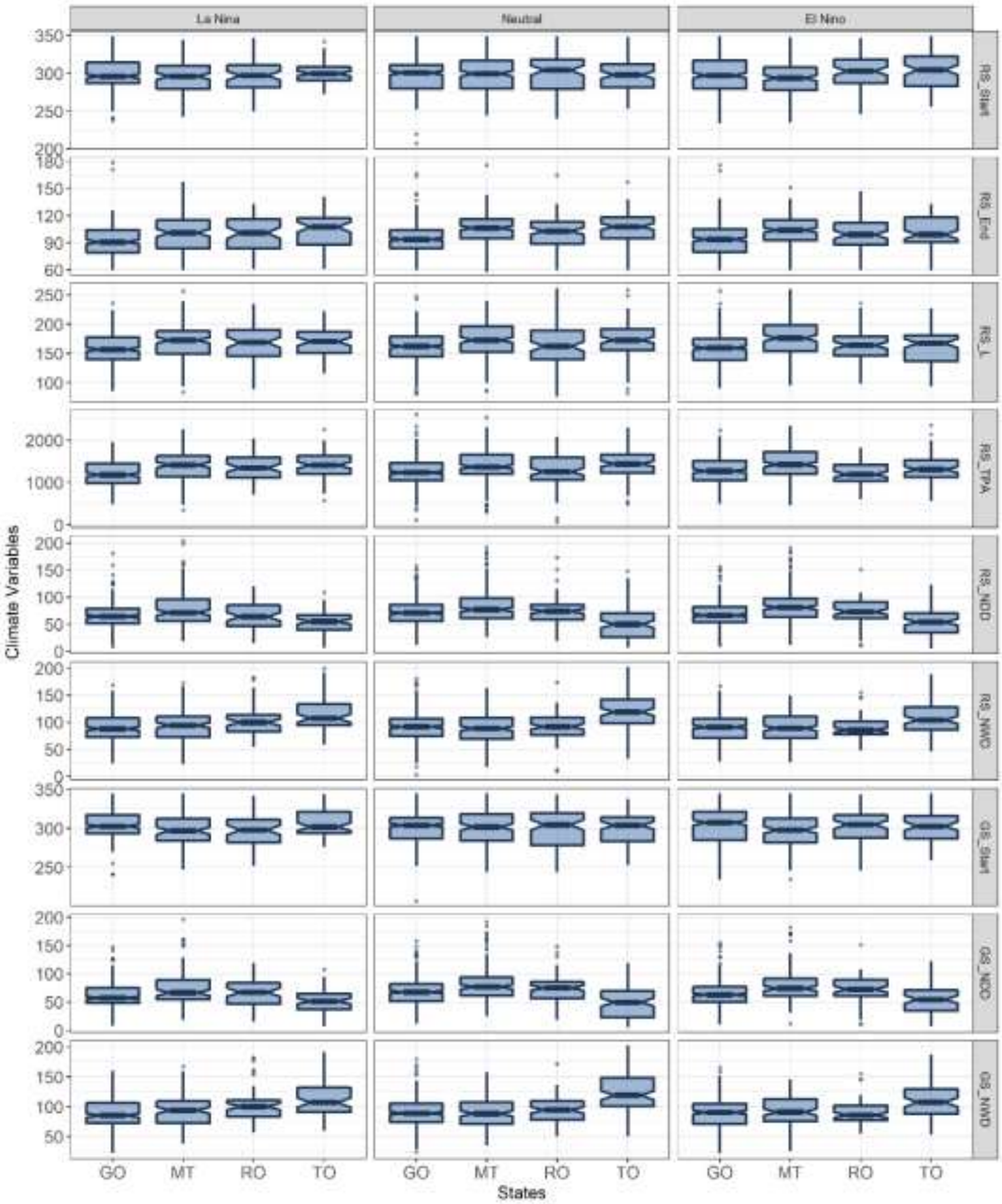

Figure 5. Boxplots highlighting the variability of climate variables (names in the panel right) in response to ENSO (La Niña, Neutral, and El Niño years (top panel)) for each state. The rainy season variables include onset (day of year; RS_{START}), cessation (day of year; RS_{END}), length (number of days; R_{SL}), total precipitation (mm; RS_{TPA}), number of dry days (number of days; RS_{NDD}), and number of wet days (number of days; RS_{NWD}). The growing season variables include onset (day of year; GS_{START}), number of wet days (number of days; GS_{NWD}), and number of dry days (number of days; GS_{NDD}). The extent

of the boxes represent the 25th and 75th sample percentiles of yield, the thick horizontal line represents the median, and the whiskers extend to 1.5 times the interquartile range.

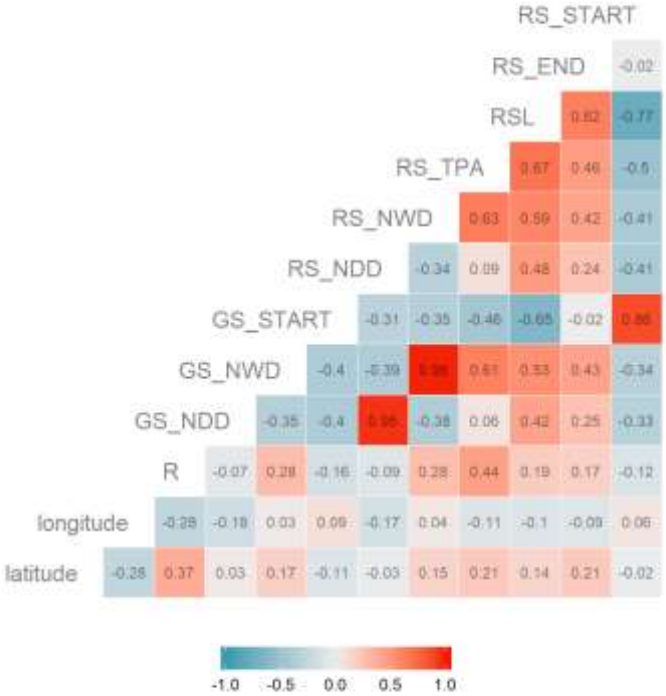

Figure 6. Spearman's rho correlations between the rainy and growing season variables. The rainy season variables include onset (RS_{START}), cessation (RS_{END}), length (RS_{L}), total precipitation (RS_{TPA}), number of wet days (RS_{NWD}), and number of dry days (RS_{NDD}). The growing season variables include onset (GS_{START}), number of wet days (GS_{NWD}), and number of dry days (GS_{NDD}). Other variables include the climatological mean annual average daily precipitation (R), longitude, and latitude.

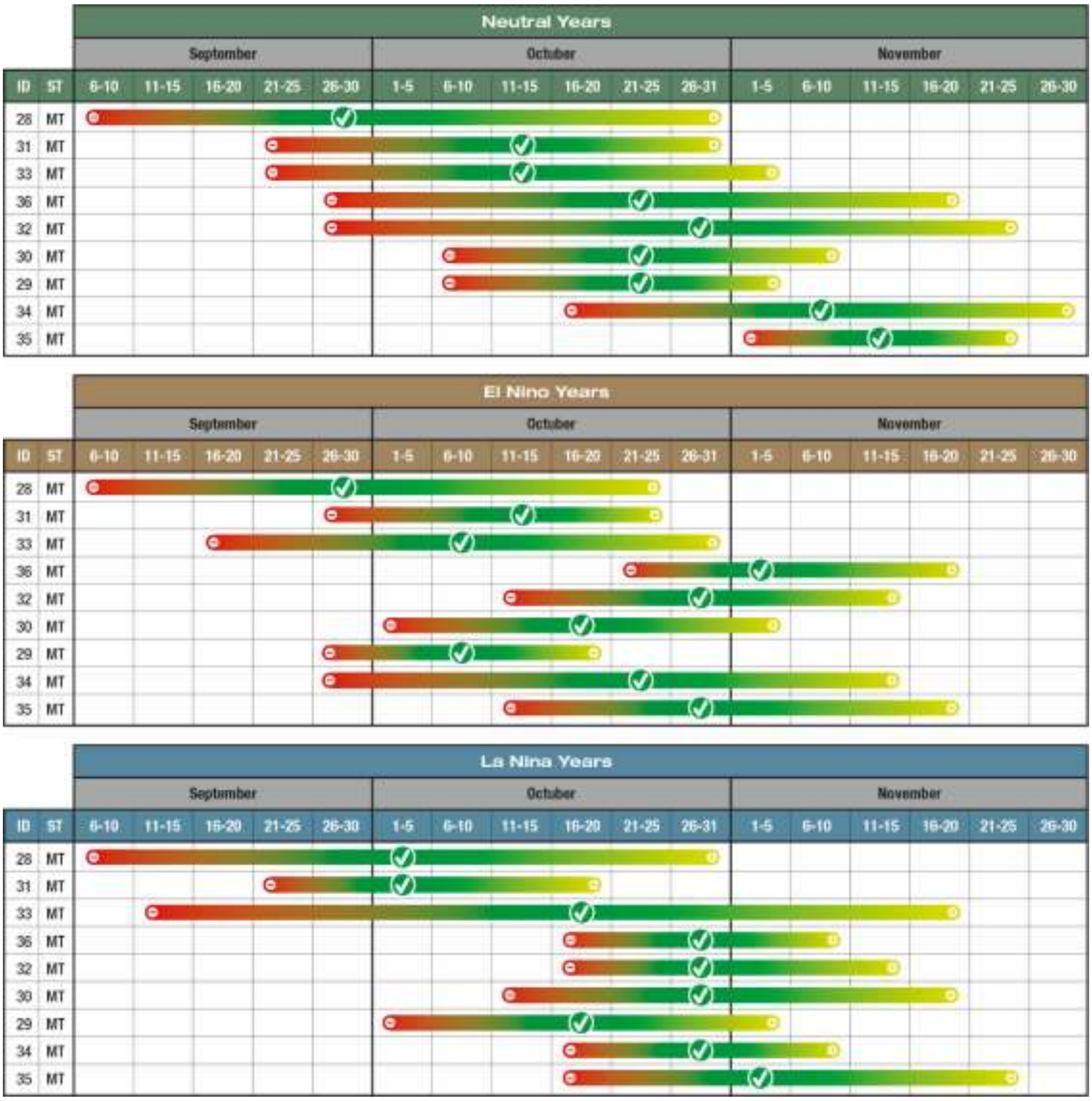

Figure 7. Crop sowing calendar for Mato Grosso State based on the growing season onset (GS_{START}) for Neutral (top panel), El Niño (middle panel), and La Niña (low panel) years. The sowing start (mean GS_{START} minus the standard deviation), mean optimal (mean GS_{START}) and end (mean GS_{START} plus the standard deviation) dates are represented by red negative circles (left), dark green checked circles (middle), and light green positive circles (right), respectively. The weather stations (ID) and states (ST) are indicated in the first and second columns. The description of each weather station ID is shown on Table 1 and Figure 1. The number of years considered Neutral, El Niño and La Niña were 13, 10 and 10, respectively.

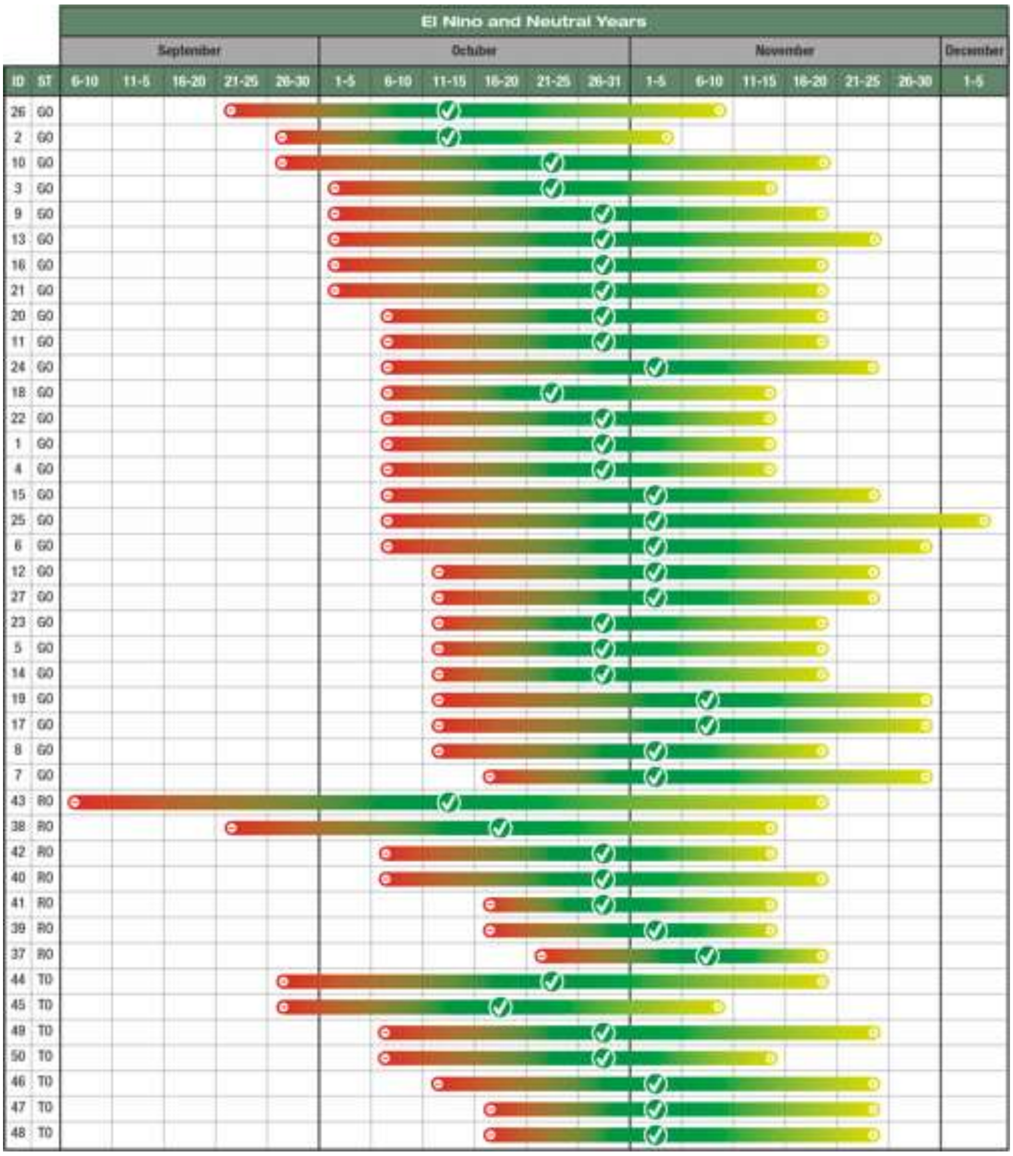

Figure 8. Crop sowing calendar for Goiás, Rondônia, and Tocantins based on the growing season onset (GS_{START}) for Neutral and El Niño years. The sowing start (mean GS_{START} minus the standard deviation), mean optimal (mean GS_{START}), and end (mean GS_{START} plus the standard deviation) dates are represented by red negative circles (left), dark green checked circles (middle), and light green positive circles (right), respectively. The weather stations (ID) and states (ST) are indicated in the first and second columns. The description of each weather station ID is shown in Table 1 and Figure 1. The number of years considered Neutral, El Niño and La Niña were 13, 10 and 10, respectively.

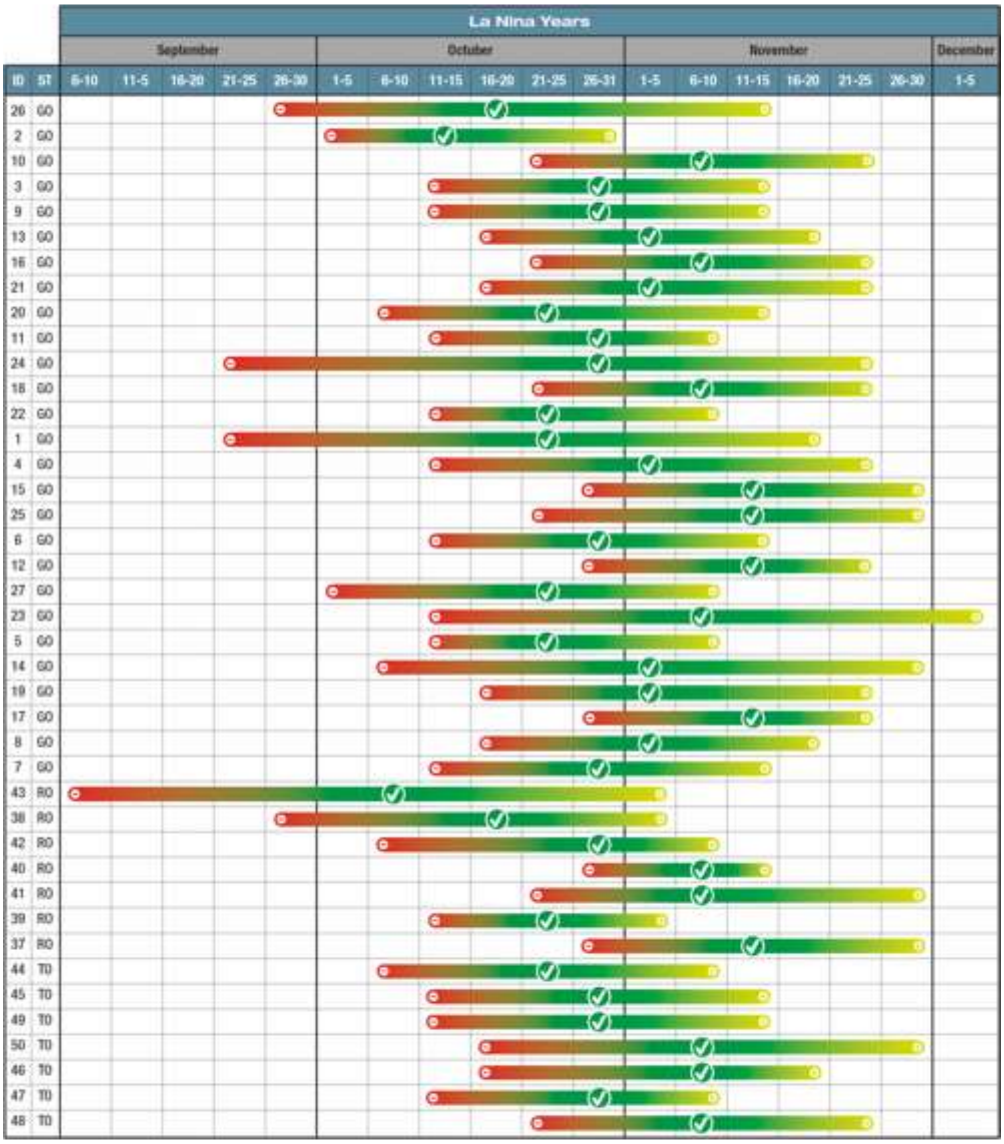

Figure 9. Crop sowing calendar for Goiás, Rondônia, and Tocantins based on the growing season onset (GS_{START}) for La Niña years. The sowing start (mean GS_{START} minus the standard deviation), mean optimal (mean GS_{START}), and end (mean GS_{START} plus the standard deviation) dates are represented by red negative circles (left), dark green checked circles (middle), and light green positive circles (right), respectively. The weather stations (ID) and states (ST) are indicated in the first and second columns. The description of each weather station ID is shown in Table 1 and Figure 1. The number of years considered Neutral, El Niño and La Niña were 13, 10 and 10, respectively